PROCEEDINGS OF SCIENCE

Pattern recognition study for different levels of UV background in JEM-EUSO experiment

Jozef Vasilko, Michal Vrabel
The Technical University of Kosice, Letna 9, 04200 Kosice, Slovakia

Pavol Bobik, Marian Putis, Blahoslav Pastircak[*†]
Institute of Experimental Physics Slovak Academy of Sciences, Watsonova 47, 04001 Kosice, Slovakia, E-mail: slavo@saske.sk

Kenji Shinozaki
Institute for Astronomy and Astrophysics, Kepler Center, University of Tubingen, Sand 1, 72076 Tubingen, Germany

Mario Bertaina, Francesco Fenu
University of Torino and INFN Torino, Torino, Italy

for the JEM-EUSO Collaboration

JEM-EUSO experiment will observe UV light created by extensive air showers initiated by ultra high energy cosmic rays (UHECR). Reconstruction of UHECR particle direction from detected signal depends also on the level of signal background, which can vary in time and with location. We developed an alternative pattern recognition (PR) method based on Hough transforms besides to existing PR methods in JEM-EUSO software framework. The results of PWISE method and Hough method were compared for the standard (nominal) UV background $500 ph/(m^2.ns.sr)$. Hough method was used to evaluation of UHECR direction reconstruction ability for higher level of UV backgrounds on the Earth's night side. The study on the impact of varying the background level on the fake trigger event rate was performed as well.

The 34th International Cosmic Ray Conference,
30 July- 6 August, 2015
The Hague, The Netherlands

[*]Speaker.
[†]A footnote may follow.

PoS(ICRC2015)661

1. Introduction

JEM-EUSO experiment will observe Earth's atmosphere from ISS orbit looking downwards to the Earth in the so called nadir mode of observation [1]. The UV light background observed continuously by JEM-EUSO detector on the Earth's night side consists from the direct and reflected components. The direct light component (airglow light) is created in the upper atmosphere. The reflected light consists from zodiacal light, integrated star light and reflected airglow light. Mainly due to airglow light production UV backgroud varies with position and time. The reflected component can contain also reflected moon light. However, JEM-EUSO observations will be performed in periods without moon light or when moon light component will be relatively small [2].

When UHECR particle very rarely hit the atmosphere and produces extensive air shower, UV light from the shower will combine with UV background to a signal registered by the JEM-EUSO detector. Discrimination of UV light created by the extensive air showers (EAS hereafter) initiated by UHECR from the UV background is important due to two main reasons. Firstly, it is important to discriminate showers photons from those created by UV background to allow precise reconstruction of UHECR characteristics. The second reason is to maximalize statistics of the registered UHECR events. Second one becomes more important when measurements face higher levels of UV background.

Discrimination of EAS photons from UV background by pattern recognition methods has a solid record in preparation history of JEM-EUSO experiment [3, 4]. Two pattern recognitions methods, PWISE [4] and the Robust method [5] were applied and the results from EAS analysis obtained by them were published.

We have developed an alternative PR method based on Hough transformation. The analysis of EAS was done in parallel by PWISE and Hough method. First for the nominal UV background $500 ph/(m^2.ns.sr)$ [6], then for different levels of UV background. Comparison of results from both methods are presented in chapter *3*.

2. Method

Photomultipliers at JEM-EUSO detector sensitive focal surface [7] is based on Multi-Anode Photomultiplier Tubes for a total of more than three hundred thousands pixels, which monitor the UV light intensity, with a time step of 2.5 μs, called GTU (Gate Time Unit). In reality triggers applied to signal will select measurements with EAS [9] [10]. For the analysis presented in this paper we used EAS generated by JEM-EUSO framework ESAF [8]. The EAS was analysed without taking trigger activation into account. Hereafter the signal from showers generated in ESAF is merged with the noise of UV background. The intensity of UV background is generated to follow the Poisson distribution with expected value λ equal to $500 ph/(m^2.ns.sr)$.

JEM-EUSO detector consists of 137 photo detector modules (PDM). Each PDM has 2304 pixels with configuration of 48x48 pixels. Detector resolution 0.075 degrees for one pixel corresponds to a $\sim 0.5 km$ on the Earth surface [11]. The shower is thus seen by couple of tenths pixels depending on energy and inclination angle of the primary UHECR particle. Only few PDMs among all the 137 working ones will see the shower during the event. Thus only PDMs where the generated shower signal appear was used for the analysis.

The analysed signal is in principle a set of pixel. There are 4 parameters describing each pixel, namely the position of pixel (x,y coordinates), the counts (brightness) registered on pixel and the time t when counts were registered. Time t is expressed by discrete values in GTU units.

We have developed two versions of algorithm for pattern recognition of EAS photons based on Hough transform. Both versions use Hough transform during the analysis several times. In following algorithm descriptions "pixel record" is record that provides unique pixel ID, pixel position on focal surface, detected photoelectron counts, GTU of recording.

Pixels from pattern recognition methods are passed to ESAF reconstruction module to find incident angles and energy of primary UHECR particle.

2.1 Method Hough 1

The first version of algorithm named Hough 1 selects pixels in two phases. To utilize this method efficiently, two thresholds are needed to be configured for analyzed UV background.

Phase 1. - Selection of shower pattern From all input pixel records for each pixel ID, pixel record with GTU with the highest number of counts is considered. Number of counts has to be above pre-defined threshold *(Pattern threshold)*. If it is not, no GTU record is selected for such a pixel ID. Hough transform is applied on these pixel records on the plane XY (plane defined by axes **x** and **y**) of detector focal surface and is used to select pixels (with unique ID) on a line with the highest sum of counts (line has "width" configuration parameter).

Phase 2. - Selection of pixel records from all GTU From all input pixel records above threshold *(Data threshold)*, only those are selected which ID is present in pixel records selected in Phase 1. Hough transform is applied to select pixels on a line with the highest sum of counts on the plane XT (defined by axes **x** and **GTU**). Similarly, Hough transform on plane YT (defined by axes **y** and **GTU**) is applied on the result of selection on the plane XT. Pixels on a line with the highest sum of counts are selected as result of this method.

2.2 Method Hough 2

Second algorithm named Hough 2 is less straightforward than Hough 1. It can be divided into three phases.

Phase 1. - Selection of shower's core pixels From all input pixel records for each pixel ID, pixel record with GTU with the highest number of counts is selected. Pixel records with counts above computed threshold are selected. This threshold is connected to number of pixels needed for pattern recognition. Neighbouring pixels in the plane XY with the highest sum of counts from this set are added weight to be preferred within this phase. Hough transform in the plane XY is applied on these pixel records with counts above the threshold to find a line with the highest sum of counts (including weights). Then 3D Hough transform in space XYT (similar to Phase 2 of method Hough 1) is applied on pixel records in an area around the line (weights are not included). Selected line of pixels is filtered to contain only neighbouring pixels that have limited maximal relative distance. Rectangle around this set of pixels is selected from all input pixel records.

Phase 2. - Selection of pixel records from all GTU 3D Hough transforms in space XYT are applied on pixel records around rectangle selection from the selection of shower's core. The transforms are applied separately for each counts value over pre-defined threshold. The ranges of angles defining Hough space are ranges of a line with the highest sum of counts selected by Hough transform from previous iteration with higher counts. Starting range is from shower's core Hough transform. Sets of pixel records selected by the use of these transforms are joined to final set.

Phase 3. - Filtration Additionally, the filtration rules based on shower characteristics were defined to reduce number of pixel records with redundant GTU. The rules are applied to each set of pixel records with the same ID. Pixel counts must be increasing with increasing GTU up to the GTU with the highest counts followed by a decreasing phase. GTU values of pixel records must be continuous. Uninterrupted sequence containing pixel records with the highest counts and the highest number of pixel records is selected.

3. Shower analysis results

For all applied pattern recognition methods we use the same set of generated data. Pattern recognition is in ESAF followed by the part of angular reconstruction process [4]. Angular reconstruction evaluates incident angles of particle θ and ϕ from the signal selected by pattern recognition method.

We have simulated over *2000* showers for each selected incident zenith angle θ. Showers positions were generated uniformly in the detector FoV. The incident zenith angles θ of the generated sets of primary UHECR protons starts at 30° with a step of *5* degrees till 75°. Energy of primary particle was set to 10^{20} eV for all simulated events.

For each shower we evaluate separation angle γ, which is defined as a difference angle between the reconstructed shower axis (determined by θ_{reco} and ϕ_{reco}) and the injected shower axis (determined by θ and ϕ of primary particle). Then we evaluate γ_{68} parameter from all γ. It is the value by which the cumulative distribution of γ reaches 0,68.

In the figure 1. we present the comparison of PWISE and both Hough based methods results. Reference PWISE results are taken from [5]. Dependency of γ_{68} separation angle on zenith angle θ for nominal background is shown. PWISE used as the reference method here provides less precise estimation of particle incident angle θ in angles bellow 65 degrees for Hough 1 method. Hough 2 method is more precise than PWISE in all angles.

Not all simulated events were reconstructed. In this analysis angular reconstruction module accepted only patter recognition results with at least 10 pixel records. Number of reconstructed events is shown in figure 2.

For protons with zenith angle 30 degrees we evaluate γ_{68} separation angle of reconstructed events for series of background levels. Starting from the nominal background $500ph/(m^2.ns.sr)$ up to $5000ph/(m^2.ns.sr)$ with step of $500ph/(m^2.ns.sr)$. In figure 3. the results from Hough 1 and Hough 2 methods are shown. Separation angle γ_{68} is increasing with the background level increase. γ_{68} rise roughly 30 percent when background increase 10 times.

From Figure 3. one can conclude that Hough 1 and Hough 2 are similarly good in events reconstruction at different background levels. However, second parameter besides γ_{68} which should

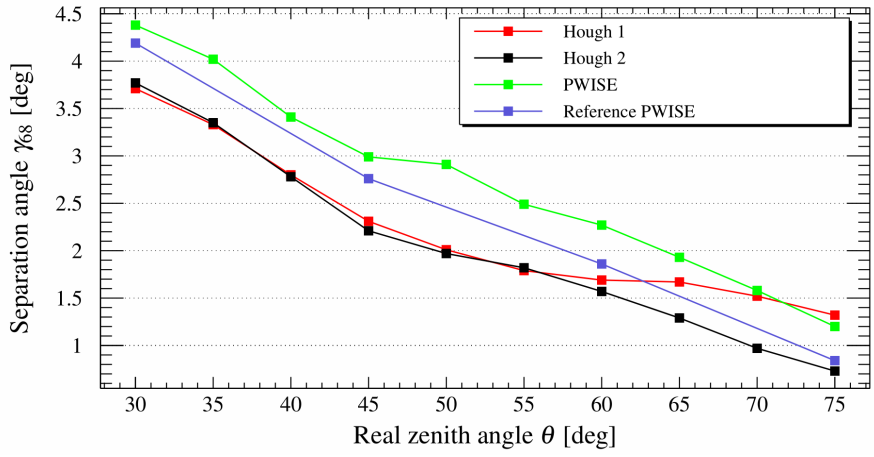

Figure 1: Separation angle γ_{68} for the energy 10^{20} eV (see text)

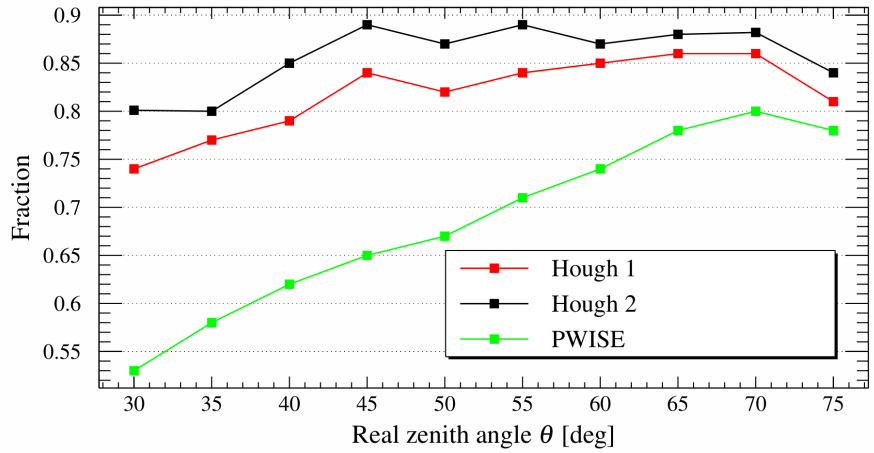

Figure 2: Fraction of reconstructed events of energy 10^{20} eV (see text)

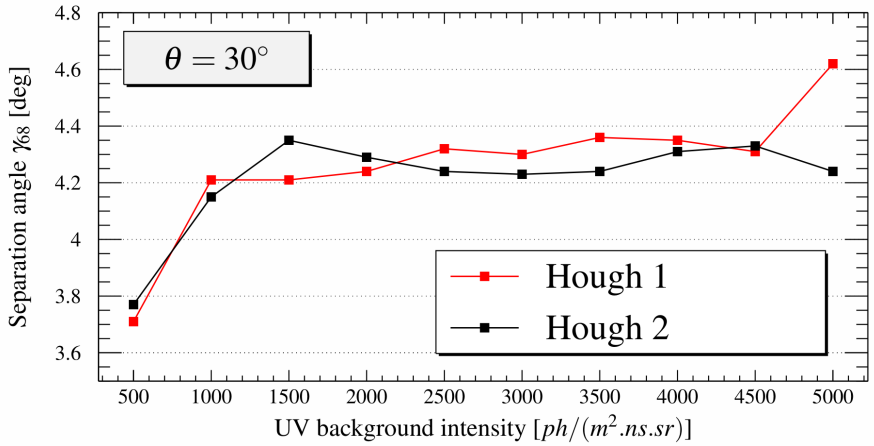

Figure 3: Separation angle γ_{68} of reconstructed events for different background levels (see text)

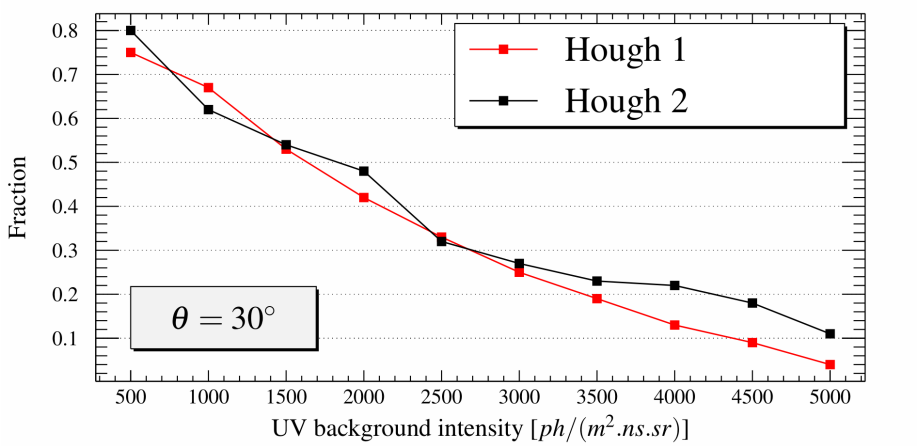

Figure 4: Fraction of reconstructed events for $\theta = 30°$

be taking into account is the number of reconstructed events. In figure 4. we observe, as expected, that the number of reconstructed events decrease with increasing level of UV background. Fraction of reconstructed events is presented for zenith angle $\theta = 30°$. Here Hough 2 resulted fractions are better than Hough 1 method results mostly at higher backgrounds.

At the end of result discussion let us stress that by lowering the quality of arrival direction determination would allow to reconstruct a higher fraction of events.

4. Trigger thresholds setup

The role of the trigger is to select EAS events greatly ejecting the random background. To reject background hits, JEM-EUSO electronics operate with several trigger levels. The system trigger works on the statistical properties of the incoming photon flux in order to detect the interesting events hindered in the background, basing on their position and time correlation. The Table 1 gives a possible reduction of the trigger rates (TR) that could be achieved at various trigger levels [12], [13].

Level	**TR at PDM level [Hz]**	**TR at FS level [Hz]**
1^{st} (PDM) Persistency trigger	~ 7	$\sim 10^3$
2^{nd} (PDM cluster) Linear track trigger	$\sim 6.7 \times 10^{-4}$	$\sim 10^{-1}$
UHECR expected rate	$\sim 6.7 \times 10^{-6}$	$\sim 10^{-3}$

Table 1: The trigger rate reduction on different trigger levels

The 1^{st} trigger level mainly operates to remove most of the background fluctuations by requiring a locally persistent signal above over a few GTU's duration. In the 1^{st} level trigger - PTT (Persistency Track Trigger) are the pixels grouped in boxes of 3×3. A trigger is issued if for 5 consecutive GTU's there is at least one pixel in the box with an activity higher than a preset threshold and the total number of detected photoelectrons in the box is higher than a preset value. These

two values are set as a function of the average noise level in order to keep the rate of triggers on fake events at a few Hz per PDM.

The role of the 2^{nd} trigger level - Linear Track Trigger (LTT) is to find some tracks segments in three dimensions from the list of pixels provided by the first level, for each GTU time bin. The track speed has to be compatible with a point travelling at speed of light in whatever direction it propagates. So it follows the movement of the EAS spot inside the PDM over some predefined time, to distinguish this unique pattern of an EAS from the background. From a PTT trigger, the PDM electronics will send a starting point, which contains the pixel coordinates and the GTU which generated the trigger. The LTT algorithm will then define a small box around it, move the box from GTU to GTU and integrate the photon counting values. When the excess of integrated value above the background exceeds the threshold, an LTT trigger will be issued. The background-dependent threshold on the total number of counts inside the track is defined to reduce the level of fake events to a rate of 0.1 Hz per FS. These two trigger levels combined together reduce therefore the rate of signals on the level of 10^9 at PDM level.

The threshold levels for triggers have to be adjusted to fit within the permissible fake TR by a large amount of background simulations. We have simulated this trigger algorithm for the PDM configuration as described in section 2 at various background levels to setup trigger thresholds in such a way, that fake TR will be reduced to above stated wished value.

Simulations have been performed for various background levels starting at $300 ph/(m^2.ns.sr)$ crossing the nominal background of $500 ph/(m^2.ns.sr)$ up to $1500 ph/(m^2.ns.sr)$. In Table 2 preliminary threshold values for PTT and LTT trigger for only several background levels close to nominal background value are shown. It has to be noted that the thresholds on the integration depend also on the thresholds at pixel level, which increase with background increasing. It has to be foreseen in the trigger scheme for each background level separatelly.

Bckg level [$ph/(m^2.ns.sr)$**]**	300	400	500	600	700
PTT threshold [*counts***]**	100	110	115	130	142
LTT threshold [*counts***]**	39	45	52	56	60

Table 2: Thresholds for PTT and LTT triggers

5. Conclusions

We developed two new pattern recognition methods for signal discrimination of EAS photons created by UHECR particles in JEM-EUSO experiment measurements. Angular reconstruction with results from methods based on Hough transform shows slightly better results than other methods used till now in the case of nominal background.

New methods were for first time applied to angular reconstruction in cases with higher UV background. Results shows that also in situations with higher background we are able to do angular reconstruction in region inside or very close to asked mission requirements. Price for it is decreasing number of successfully reconstructed events with increasing background.

Acknowledgment: This work was partially supported by Basic Science Interdisciplinary Research Projects of

RIKEN and JSPS KAKENHI Grant (22340063, 23340081, and 24244042), by the Italian Ministry of Foreign Affairs, General Direction for the Cultural Promotion and Cooperation, by the 'Helmholtz Alliance for Astroparticle Physics HAP' funded by the Initiative and Networking Fund of the Helmholtz Association, Germany, and by Slovak Academy of Sciences MVTS JEM-EUSO as well as VEGA grant agency project 2/0076/13. Russia is supported by the Russian Foundation for Basic Research Grant No 13-02-12175-ofi-m. The Spanish Consortium involved in the JEM-EUSO Space Mission is funded by MICINN & MINECO under the Space Program projects: AYA2009-06037-E/AYA, AYA-ESP2010-19082, AYA-ESP2011-29489-C03, AYA-ESP2012-39115-C03, AYA-ESP2013-47816-C4, MINECO/FEDER-UNAH13-4E-2741, CSD2009-00064 (Consolider MULTIDARK) and by Comunidad de Madrid (CAM) under projects S2009/ESP-1496 & S2013/ICE-2822.

References

[1] J.H. Adams Jr. et al. - JEM-EUSO Collaboration, *Astroparticle Physics* **44** (2013) 76

[2] P. Bobik et.al. - JEM-EUSO Collaboration, *Proceedings of the 13th ICATPP Conference* (2012) 19

[3] M. Bertaina et al. - JEM-EUSO Collaboration, *Advances in Space Research* **53** (2014) 1515

[4] A. Guzman et al. - JEM-EUSO Collaboration, *Journal of Physics: Conference Series* **409** (2013) 012104

[5] S. Biktemerova, A. Guzman, T. Mernik, *Experimental Astronomy, Online First* 2014 10.1007/s10686-013-9371-0

[6] P. Bobik et al. - JEM-EUSO Collaboration, *Proceedings of the 32nd ICRC* **3** (2011) 188

[7] Y. Kawasaki et al. - JEM-EUSO Collaboration, *Astrophys. Space Sci. Trans.* **7** (2011) 167

[8] C. Berat et al., *Astroparticle Physics*, **33** (2010) 22

[9] I. Park et. al. - JEM-EUSO Collaboration, *Proceedings of the 32nd ICRC* **3** (2011) 305

[10] J. Bayer et. al. - JEM-EUSO Collaboration, *Proceedings of the 33rd ICRC* (2013)

[11] A. Haungs - JEM-EUSO Collaboration, *The JEM-EUSO Mission: Contributions to the ICRC 2013* (2013) arXiv:1307.7071

[12] J. Bayer et. al. - JEM-EUSO Collaboration, *Proceedings of the 32nd ICRC* **3** (2011) 168

[13] J. H. Adams Jr. et al., *Summary Report of JEM-EUSO Workshop at KICP, Chicago.* arXiv:1203.3451v1